Proc. Natl. Acad. Sci. USA
Vol. 92, pp. 8616–8620, September 1995
Neurobiology

Cortical activity flips among quasi-stationary states

(single-unit activity/behaving monkeys/hidden Markov models)

MOSHE ABELES*†, HAGAI BERGMAN*, ITAY GAT‡, ISAAC MEILIJSON§, EYAL SEIDEMANN§, NAFTALI TISHBY‡, AND EILON VAADIA*

*School of Medicine and Center for Neural Computation, Hebrew University, P.O. Box 12272, Jerusalem 91120, Israel; ‡Institute of Computer Science and Center for Neural Computation, Hebrew University, Jerusalem 91904, Israel; and §School of Mathematical Sciences, Raymond and Beverly Sackler Faculty of Exact Sciences, and School of Medicine, Tel Aviv University, Tel Aviv 69978, Israel

Communicated by L. R. Rabiner, AT&T Bell Laboratories, Murray Hill, NJ, May 1, 1995

ABSTRACT **Parallel recordings of spike trains of several single cortical neurons in behaving monkeys were analyzed as a hidden Markov process. The parallel spike trains were considered as a multivariate Poisson process whose vector firing rates change with time. As a consequence of this approach, the complete recording can be segmented into a sequence of a few statistically discriminated hidden states, whose dynamics are modeled as a first-order Markov chain. The biological validity and benefits of this approach were examined in several independent ways: (*i*) the statistical consistency of the segmentation and its correspondence to the behavior of the animal; (*ii*) direct measurement of the collective flips of activity, obtained by the model; and (*iii*) the relation between the segmentation and the pair-wise short-term cross-correlations between the recorded spike trains. Comparison with surrogate data was also carried out for each of the above examinations to assure their significance. Our results indicated the existence of well-separated states of activity, within which the firing rates were approximately stationary. With our present data we could reliably discriminate six to eight such states. The transitions between states were fast and were associated with concomitant changes of firing rates of several neurons. Different behavioral modes and stimuli were consistently reflected by different states of neural activity. Moreover, the pair-wise correlations between neurons varied considerably between the different states, supporting the hypothesis that these distinct states were brought about by the cooperative action of many neurons.**

While early sensory and late motor processes can be carried out in parallel, many intermediate processes are carried out serially (1–4). Our own introspective experience tells us that our thought processes evolve serially one after the other. Some current models of neural networks (5–7) also suggest a series of quasi-stable states which follow each other in succession.

Usually, the analysis of the activity of single neurons is done by looking at their firing rates in relation to some external marker, such as a visual stimulus or a movement. In the work presented here, we treat the activity of several single neurons, which were recorded in parallel, as a spike-count vector—i.e., a vector whose first component is the number of spikes generated by the first neuron in a given time window, the second component is the spike count of the second neuron in the same window, and so forth.

Until recently, almost no attempt was made to search for experimental evidence that the brain, or some part of it, goes through a sequence of distinct states.¶ In the present work we examined whether spike count vectors can be regarded as the output of a hidden Markov process which switches among discrete states of underlying collective activity.

The HMM is a well-known technique of stochastic modeling used so far mostly for speech and handwriting recognition (10). Within this model, the observations are considered as stochastic functions of a Markov process whose states are "hidden"—i.e., not directly observable. There are well established ways of estimating the model's parameters from training data, as well as evaluating the probability of test data being generated by the model. The model produced can also be used to impose temporal segmentation on the data.

In the present context, the observations are the recorded neural spike trains, whereas it is claimed that the emerging states correspond to some underlying organization of the local cortical activity. Our results show not only that such treatment is possible but that it yields states which are specific to the external events and to their behavioral significance and exhibit distinct interaction patterns between the neurons. Preliminary reports of some of the results described here were presented in refs. 11 and 12.

EXPERIMENTAL METHODS

Firing times of neurons were obtained in experiments on localization and short-term memory for space. In these experiments, monkeys were trained to localize a source of light blink and then, after a delay, to touch the target from which the light blink was presented. The monkeys started a trial by touching a ready key, then the central ready light was turned on. Three to six seconds later, a visual cue was given in the form of a 200-ms light blink coming from either the left or the right. Then, after a delay of 1–32 s, the color of the ready light changed from red to orange (the GO signal), and the monkeys had to release the ready key and touch the target from which the cue was given. Correct responses were reinforced by a drop of juice. This paradigm was called the GO mode. In this mode, the monkeys almost always fixed their gaze on the ready light in the first 4 s. As a control, the monkeys were also trained to perform a different paradigm in which all the events were identical to those of the GO mode, except that after the GO signal the monkeys had to refrain from responding. This paradigm was referred to as the NO-GO mode.

The monkeys were trained to switch between modes when a set of lights was turned on for 3–4 s. Modes were switched after four correct trials. In this way, one could study the relation between brain activities and stimuli in two different "sets of mind."

When the monkeys were fully trained (over 90% correct performance), they were anesthetized and prepared for re-

The publication costs of this article were defrayed in part by page charge payment. This article must therefore be hereby marked "*advertisement*" in accordance with 18 U.S.C. §1734 solely to indicate this fact.

Abbreviations: HMM, hidden Markov model; PSTH, poststimulus–time histogram; NHPM, nonhomogeneous Poisson model.

†To whom reprint requests should be addressed.

¶While this report was being written, Radons brought to our attention his work on hidden Markov model (HMM) analysis of spike trains from the visual cortex of anesthetized monkeys (8). Another application of HMM to neural activity (9) deals with the excitability changes which follow a spike in a single neuron.

cording of single-unit activity from the frontal areas around the upper limb of the arcuate sulcus. These areas receive connections from the somatosensory, the visual, and the auditory areas and affect the motor areas (13, 14). In previous studies, we found that over 40% of the units in these areas modulate their firing rates in relation to one or another aspect of this task. Electrodes for recording eye movements were also implanted during this operation.

Upon recovery and retraining, activity was recorded daily while the monkey performed the task.[‖]. The results reported here are based on data from two monkeys. On every recording day, the simultaneous activity of 6–16 single units was recorded through six metal microelectrodes. The horizontal distance between electrodes was 0.5–1.0 mm. The monkeys' care and treatment were in accordance with the regulations of the National Institutes of Health and the Hebrew University.

METHODS OF ANALYSIS

The vector of parallel, recorded spike trains was regarded as the output of an HMM. Given the number of hidden states, the parameters of the model are the Markov state transition probabilities and the joint distribution of the spike trains at each hidden state (8, 11). We assume that in every hidden state the spike trains are independent, stationary Poisson processes and that their state conditional distribution is specified by a vector of firing rates. Fig. 1 illustrates this idea.

The HMM analysis allowed us to estimate these parameters via the identification of a most likely hidden Markov process that fits the recorded data. Using this trained model, we obtained estimates of the probability of the system being in any possible state at each point in time. The most probable sequence of states obtained in this way provided a segmentation of the data.

Two methods of reconstructing an HMM from the recorded data were examined. The goal of the first (supervised) method was to identify and characterize the sequence of states which followed a known external stimulus. The purpose of the second (unsupervised) method was to parse the entire recorded data without any specific reference to the external events.

The supervised analysis considered only the first 4 s of activity during the delay which followed the spatial cue—a light blink from the left or from the right. Typically, 70 repetitions of the same stimulus were submitted to analysis. In this analysis, we utilized a fine time resolution of 1 ms. The activity of each neuron (firing or quiescent) at each millisecond was considered as the output of the process. The Baum–Welch algorithm (15) was used to estimate the state transition probabilities and the expected spike rates of each neuron in each state.

The modulations of firing rates of each neuron, following each of the four stimuli, were evaluated by means of post-stimulus–time histogram (PSTH) with variable bin sizes. The PSTH is an estimator of the time-variable firing rate of a neuron (16). The bin size of the PSTH was not fixed, as is customary, but varied so as to contain 100 spikes per bin. This yields a constant accuracy of estimation of the rates, at the price of losing time resolution when the firing rates are low.

The unsupervised HMM was based on the measured, local spike count of each neuron, obtained by sliding a 500-ms window at 100-ms steps over all the data. Thus, training of this model was carried out in a coarse time resolution. The spike counts of all the neurons at any given instant within the 500-ms window were considered as the vector output of the process. By using the Baum–Welch algorithm, the HMM state parameters (spike-rates vector) and state-transition probabilities were estimated. This algorithm also provided the most likely segmentation of the data into states (11).

[‖]We stress that this report does not relate to the process of learning anything new, but to the sequence of states through which the neural networks (in which the recorded neurons might be embedded) pass, while the monkey performs a task with which it is familiar.

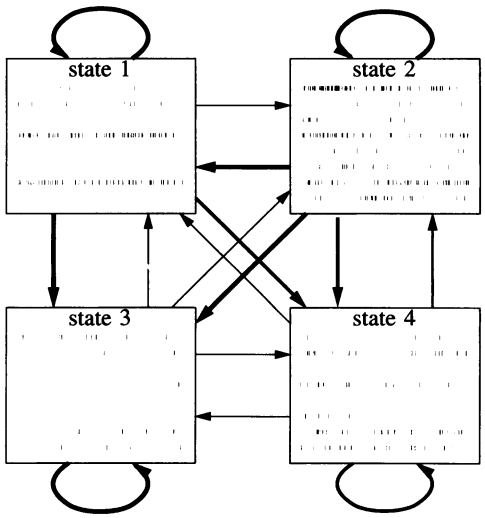

FIG. 1. Schematic description of a first-order HMM for the firing rates. The system can be in one of four states at any given time step, and its transition probabilities depend only on the current state. These transition probabilities are represented in the diagram by the thickness of the corresponding arrows. Samples of 4 s of observed firing patterns of the eight neurons at every state are illustrated inside each box. Notice that the states are characterized by the list (vector) of eight firing rates and that no single unit can discriminate among the states. All we observe about the system are the firing times of the neurons, and from these observations we wish to reconstruct the complete HMM.

RESULTS AND DISCUSSION

In this section we describe the results of several different methods of analysis carried out in this work: (*i*) Segmentation of the cortical activity. This was performed both in the local, fine-resolution, supervised method and the global, coarse time resolution, unsupervised method. We tested the significance of the observed, sharp state flips by using surrogate data. (*ii*) Prediction of behavior. Models trained on every one of the four different behavioral modes following the cue (GO/NO-GO, Left/Right) were tested for prediction of the actual behavior of the monkey. Comparison of the HMM with the nonhomogeneous Poisson model (NHPM) is also reported. (*iii*) Direct measures of the collective cortical transitions. We independently verified the sharp transitions exhibited by the HMM analysis, both for the supervised (local) and unsupervised (global) methods. (*iv*) Pair-wise cross-correlations. We examined the pair-wise cross-correlations in each of the segmented states and found that the correlation varied from state to state. This analysis was performed on segments labeled by the coarse-time resolution method.

As in most other applications of HMM, the number of states of the Markov process was determined through trial and error to obtain good performance under a relatively low-dimensional parameter model. In the framework of this study, 28 different data segments were subject to the HMM analysis. In all 28 cases analyzed, use of six to eight states of the HMM was sufficient to discriminate among the different modes and stimuli. Using more states did not provide any better discrimination and required more training data.

It should be noted that no claim is being made concerning any biological significance of the obtained number of states. The number of states is merely a consequence of the quality and duration of the recorded data. The obtained segmenta-

tion, however, reflects a coarse-grained picture of the underlying cortical dynamics.

The significance of the obtained state sequence was verified by the consistency of the procedure. Essentially the same states and segmentations were obtained when the model was trained on different (non-overlapping) portions of the recording day and from different random initial conditions.

Segmentation of Cortical Activity

Once the model was constructed, it was possible to segment the activity which followed a single stimulus presentation (Fig. 2*A*) into a sequence of states. Fig. 2*B* illustrates the segmentation obtained with the supervised method, and Fig. 2*C* illustrates the segmentation of the same data by the unsupervised method. Due to the coarse time resolution of the second method, the transitions in state probabilities were not as sharp as in the first method, but the same states apply globally to all the data and not just locally, following the visual cue.

Both algorithms did indeed parcel the activity into time segments which belonged to different states. Notice that the transitions were sharp and that there was almost always one state which was much more probable than the others. The steep transitions seen in Fig. 2*B* genuinely support the idea of fast flips from state to state. In most cases, the sharp transitions were not due to a change of activity of a single neuron but to a change in the vector activity of several units. This emphasized the benefits of our vector signal-processing approach.

Is this sharp flipping from state to state (Fig. 2*B*) a real property of the data or an artifact of the HMM algorithms? This question was considered by applying the fine-time-resolution HMM analysis to surrogate spike trains, obtained by simulating the spike trains as nonhomogeneous Poisson processes with 1-ms refractoriness. The time-variable firing rates in the simulation were those obtained by the PSTH of the real data.

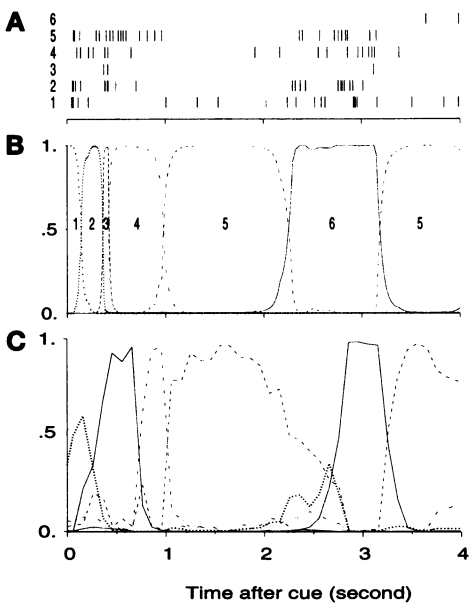

FIG. 2. (*A*) Firing times of six neurons during 4 s after a light blink from the right. A total of 93 trials of this kind (excluding the one shown here) were used to construct an HMM which maximizes the likelihood of the observed activity. (*B*) Probabilities of being in any one of the six states of the model given the spiking times shown at the top. Parameter estimation was carried out under the supervised method. (*C*) Similar segmentation of the same data, according to a model constructed by the unsupervised method. The similarity between the two segmentations is an indication of the "global" nature of the states.

In the real data, the states flipped 1–3 times every second. Sixty-nine percent of the time, the current, most likely state had a probability above 0.8. In the surrogate data, the probability was above 0.8 for only 21% of the time. Thus, the sharp transients and high probabilities of one of the states, as seen in Fig. 2*B*, are a genuine property of the data and not a by-product of the HMM analysis.

Prediction of Behavior

To assess the specificity of the supervised HMM to the monkeys' behavior, we constructed supervised HMMs for data after the blink from the right or the left. This was done for both the GO and the NO-GO modes. Each trial, in its turn, was excluded from the training data, and then its likelihood under the four models was evaluated (10). When the obtained likelihood was highest for the model trained in the appropriate category, we considered the classification successful.

The data included only 4 s of activity which followed the visual cue and preceded the monkeys' response. Nevertheless, the HMM predicted these responses in 987 of the 1099 trials in which the monkeys responded correctly. When the likelihood of the 99 trials in which the monkey actually made an error was estimated, the HMM could predict the monkey's failure in 46 cases. In summary, the HMMs trained for the four data classes could predict the true reaction of the monkey in each trial with 90% accuracy.

Is the predictive power of the HMM better than what might be obtained with standard methods used by physiologists? To answer this question, the modulations of firing rates of each neuron following each of the four stimuli were evaluated by means of the PSTH, which described the data as a NHPM with deterministic rates. Once more, the likelihood of the data of each trial was estimated under the four NHPMs and classification was carried out according to the maximum likelihood model. In this method, the correct responses could be predicted for 990 trials. The NHPM could predict erroneous responses for 35 trials of the 99 actual errors. Thus, the NHPM could predict the monkeys' response just as well as the HMM.

The two models presented here, the NHPM and the HMM, are similar when the activity of only one neuron and one type of stimulus are considered. Although the two models look very different, one corresponds to deterministic changes in firing rate, and the other to stochastic changes, they are essentially the same in some limit. In a hidden Markov process with a large number of states and unidirectional transitions, the transitions are almost continuous and deterministic, essentially as in a nonhomogeneous Poisson process. This is how Radons *et al.* (8) treated their experimentally recorded visual activity. On the other hand, a nonhomogeneous Poisson process in which the underlying rate function is allowed to have a variable delay of onset and whose duration and amplitudes can be squeezed or stretched (time and amplitude warping) could well accommodate data that are generated by a hidden Markov process. The method of choice depends on the hypotheses about the underlying cortical processes and on parsimony. With the type of data presented here, the HMM adequately explained the data with smaller number of parameters.

The analysis of the data that followed the visual cue supports both the notion of discrete states, better captured with the HMMs, and the notion of continuous dynamics, for which the PSTH analysis is more appropriate. The first second or so after a discrete stimulus is marked by rapid modulations of firing rates which are locked in time to the stimulus. For this period, the PSTH analysis is appropriate. However, later on, when the activity indicates sharp transitions among quasi-stationary states with very poor time locking to the stimulus (such as the transitions between states 5 and 6 in Fig. 2), the HMM is more appropriate. Moreover, the HMM analysis indicates that the

same states consistently reappear during most of the recorded activity, not just in the first seconds following the stimulus.

Collective Cortical Transitions

The HMM is clearly advantageous in its ability to handle the multielectrode recording as a vector Poisson process. The advantage of the joint processing of the simultaneous firing rates of all the neurons by the HMM is demonstrated in the data shown in Fig. 2. Careful examination of the firing patterns of neurons 2 and 5 in the top figure reveals that the spike counts of both neurons were altered together around the first and third seconds. Such comodulations of the spike patterns are a hallmark of the vector Markov process.

To test the generality of this observation, we treated transitions between states as stimuli and computed the PSTHs of the unit activity around these points. This analysis was carried out first for the transitions revealed by the fine-time-resolution (1 ms) method. Since the firing modulations within the first second after the cue could be also described adequately by assuming a nonhomogeneous Poisson process, we concentrated on transitions occurring between the second and fourth seconds after the stimulus. In this period, the average firing rate of the accumulated PSTH was constant.

Fig. 3 *A* and *B* illustrates this type of analysis. They show that the firing rates of neurons 1, 2, 4, and 5 changed concomitantly around the transition from state 5 to state 6. Neurons 3 and 6 did not alter their firing rates around this point of transition and are thus not shown. The noisy nature of the firing process and the low firing rates (below 10 Hz) dictated the usage of a 20-ms-wide bin for constructing the PSTHs. Thus, the apparent transition time of 20–40 ms should be regarded as an upper bound.

Another advantage of the HMM is its ability to segment the entire data stream into states with similar activity in an unsupervised manner—i.e., without any knowledge of stimuli or movement times. Unlike the PSTH analysis (based on the NHPM), where the statistics come from the alignment of many different recordings by the external stimulus, the unsupervised HMM can collect information from various parts of the recording, irrespective of their location relative to the stimuli.

The coarse-time-resolution method used a 500-ms window, which was advanced in 100-ms steps. Therefore, it cannot position the transition time accurately enough. Nevertheless, we obtained a direct measure of the sharpness of the transitions from the probabilities that two adjacent data slices were generated by the same vector Poisson process, independent of the HMM analysis. We considered all the transitions between a specific pair of states and collected the spike trains of all the neurons recorded during these transitions within a range of 1000 ms (−500 ms to +500 ms). The range of the accumulated activity was broken down into slices of width 32 ms. For each neuron, there were 31 slices, and for each such slice, the average firing rate of the neuron was calculated. Using the Poissonian assumption for each neuron, we calculated the probability that the nth slice has the same statistical origin as the $(n - 1)$th slice.

It can easily be seen that close to the transition point, as marked by the HMM, the probability that the two adjacent slices are not of the same statistical origin is significantly higher than anywhere else in that region. Furthermore, this phenomenon is clearly a collective effect of most of the measured neurons and is hardly noticeable for a single neuron in this group.

Concomitant changes of firing of several neurons around the transition point were observed in all the cases examined in this way. Most frequently, all the changes of firing rates were in the same direction. Occasionally, one of the neurons decreased its firing rate while the others increased it, or vice versa.

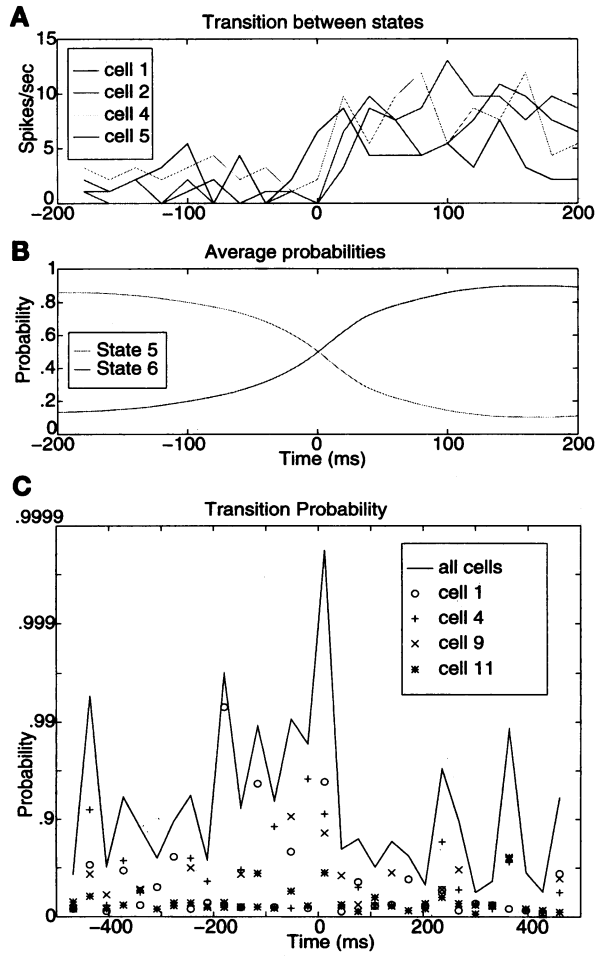

FIG. 3. Concomitant changes of firing rates around the transition from state 5 to state 6. (*A* and *B*) A total of 46 transitions from state 6 to state 5 in the GO mode following a cue from the right for which the HMM stayed at least for 200 ms in each of the states were marked as a "stimulus." A PSTH around this stimulus was computed for all the recorded neurons by using a time bin of 20 ms. The PSTHs for the four neurons that changed their firing rates around this transition are shown in *A*. The average probability of being in these two states is shown in *B*. (*C*) Probability of a transition between states 1 and 2 of the HMM is estimated directly in the coarse temporal resolution. All 374 transitions from state 1 to 2 were aligned as an event. Spike counts from −500 to +500 ms around this event were calculated in 32-ms-wide bins. The probability of transition is estimated as follows: 1 minus the probability that the counts in the nth bin originated from the same Poisson process that generated the counts in the $n - 1$ bin. This calculation was carried out separately for each neuron. Assuming (conditional) independence of the neurons, the probabilities of remaining in the same state were multiplied to obtain the likelihood of no transition at this point. The connected line is the probability of corresponding transition during this time, based on the firing of all the neurons. The different symbols represent the probabilities of transition based on the firing of individual neurons.

State-Dependent Pair-Wise Cross-Correlations

A striking evidence for the validity of the segmentation provided by the HMM are the state-dependent cross-correlations, revealed by the unsupervised segmentation (Fig. 4). The assumption that the network has different sets of organized activity was tested by studying the cross-correlations between pairs of neurons in the different states (17). The data was subjected to the coarse-time-resolution HMM analysis. Intervals in which the activity stayed in the same state for more than 1 s were pulled together, and the cross-correlations between all the pairs of neurons were computed. This type of

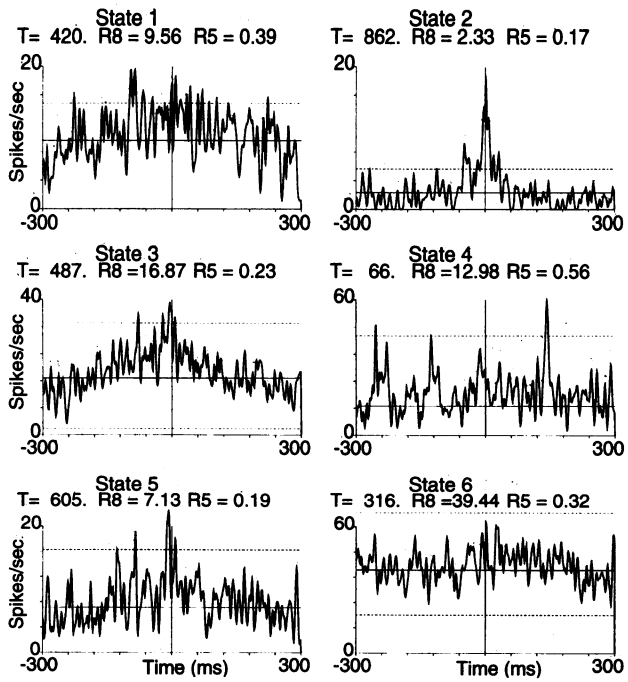

FIG. 4. An HMM with six states was constructed for all the trials in which the monkey performed according to the GO mode. Cross-correlations between neurons 5 and 8 were computed separately for each state. The graphs show the firing rates in spikes per second of neuron 8 (R8) around the time that neuron 5 (R5) fired. The dotted lines mark the band which is expected to contain 99% of the data for two, independent Poisson processes. The three numbers above each graph are the total time spent in the state and the firing rates of neurons 8 and 5. The activity of the neurons in state 6 was considered as being uncorrelated, and the graphs for states 2 and 3 indicated positive correlations between the neurons. The graph for state 4 was judged as having too little data and was not considered for further analysis. States 1 and 5 were not taken into consideration in estimating the modifiability of the cross-correlations between neurons 5 and 8 because the shapes of the cross-correlograms (flat or nonflat) could not be categorized unequivocally.

analysis was repeated for five different groups of neurons recorded on different days. Altogether, the cross-correlations among 114 pairs of neurons were computed, each in six to eight possible states. Fig. 4 illustrates the cross-correlations of one pair of neurons in different states. The limited recording time in each state (a few hundreds of seconds) and the low firing rates of most cortical neurons yield rather noisy cross-correlations. Despite this noisiness, one can observe which correlations are clearly nonflat—e.g., states 2 and 3 in Fig. 4—and which are clearly flat—e.g., state 6 in Fig. 4.

Only when a pair of neurons changed their interaction from a clearly flat to a clearly nonflat cross-correlation did we consider them as exhibiting a modifiable cross-correlation. Twenty-six pairs of neurons showed a clear peak or a trough near the origin, indicating temporal relations between the firing times of the two neurons in at least one state. For most of these pairs (25 of 26 pairs), the cross-correlation shapes were clearly related to the HMM states, showing a clearly flat correlation for some other states (Fig. 4). Thus, although the reconstruction of the HMM was based only on the expected firing rates in 500-ms windows, it also captured the dynamics of the cross-correlations among the neurons on a much finer time resolution.**

This observation strongly supports the idea that neural networks in the brain dwell most of the time in stable configurations of activity ("attractors" or "states"), each having distinct firing rates and neuronal interactions. The HMM analysis enables the researcher to reveal these internal brain states and to track the computation processes, expressed as transitions between these internal states.

**We note that a recent study of the pair-wise correlations by means of joint peristimulus histograms of the same data showed that the cross-correlations changed dynamically within 20–40 ms and are stable for periods of 200–500 ms (18).

We thank I. Haalman, Y. Prut, and H. Slovin who carried out the experiments. This research was supported in part by grants from the United States–Israeli Binational Science Foundation and the Human Frontier Science Program.

1. Triesman, A. & Gilade, G. (1980) *Cognit. Psychol.* **12,** 97–136.
2. Crick, F. (1984) *Proc. Natl. Acad. Sci. USA* **81,** 4586–4590.
3. Georgopoulos, A. P., Schwartz, A. B. & Kettner, R. E. (1986) *Science* **233,** 1416–1419.
4. Rosenbaum, D. A. (1985) in *Motor Behavior: Programming, Control and Acquisition*, eds. Heuer, H., Kleinbeck, U. & Schmidt, K. M. (Springer, Berlin), pp. 1–33.
5. Amit, D. J. (1989) *Modeling Brain Function: The World of Attractor Neural Networks* (Cambridge Univ. Press, New York).
6. Sompolinsky, H. & Kantor, I. (1986) *Phys. Rev. Lett.* **57,** 2861–2864.
7. Metzger, Y. & Lehmann, D. (1990) *Network* **1,** 169–188.
8. Radons, G., Becker, J. D., Dulfer, B. & Kruger, J. (1994) *Biol. Cybernetics* **71,** 359–373.
9. Deppisch, J., Pawelzik, K. & Giesel, T. (1994) *Biol. Cybernetics* **71,** 387–399.
10. Rabiner, L. R. (1989) *Proc. IEEE* **77,** 257–286.
11. Gat, I. & Tishby, N. (1993) *Neural Inf. Process. Syst.* **5,** 945–953.
12. Seidemann, E., Meilijson, I., Bergman, H., Vaadia, E. & Abeles, M. (1994) *Soc. Neurosci. Abstr.* **20,** 443.
13. Fuster, J. M. (1988) *The Prefrontal Cortex: Anatomy, Physiology and Neuropsychology of the Frontal Lobe* (Raven, New York).
14. Goldman-Rakic, P. S. (1987) in *Handbook of Physiology: The Nervous System*, eds. Mountcastle, V. B., Plum, F. & Geiger, S. R. (Am. Physiol. Soc., Bethesda), Vol. 5, Pt. 1, pp. 373–417.
15. Baum, L. E. & Petrie, T. (1966) *Ann. Math. Stat.* **37,** 1554–1563.
16. Gerstein, G. L. & Kiang, N. Y.-S. (1960) *Biophys. J.* **1,** 15–18.
17. Gerstein, G. L., Perkel, D. H. & Moore, G. P. (1967) *Biophys. J.* **7,** 419–440.
18. Vaadia, E., Haalman, I., Abeles, M., Bergman, H., Prut, Y., Slovin, H. & Aertsen, A. (1995) *Nature (London)* **373,** 515–518.